

SCIENTIFIC REPORTS

OPEN

Infrared Spectroscopic Evidences of Strong Electronic Correlations in $(\text{Sr}_{1-x}\text{La}_x)_3\text{Ir}_2\text{O}_7$

Gihyeon Ahn¹, S. J. Song¹, T. Hogan^{2,3}, S. D. Wilson³ & S. J. Moon¹

Received: 09 May 2016

Accepted: 11 August 2016

Published: 07 September 2016

We report on infrared spectroscopic studies of the electronic response of the $(\text{Sr}_{1-x}\text{La}_x)_3\text{Ir}_2\text{O}_7$ system. Our experiments revealed hallmarks of strong electronic correlations in the evolution of the electronic response across the filling-controlled insulator-metal transition. We observed a collapse of the $J_{\text{eff}} = 1/2$ Mott gap accompanying the transfer of the spectral weight from the high-energy region to the gap region with electron doping. The intraband conductivity at the metallic side of the transition was found to consist of coherent Drude-like and incoherent responses. The sum rule and the extended Drude model analyses further indicated a large mass enhancement. Our results demonstrate a critical role of the electronic correlations in the charge dynamics of the $(\text{Sr}_{1-x}\text{La}_x)_3\text{Ir}_2\text{O}_7$ system.

Electronic correlations have been the source of numerous exotic phenomena including metal-insulator transitions and high- T_c superconductivity in $3d$ and $4d$ transition metal oxides¹. A new frontier in the search for correlation-driven novel states is the exploration of $5d$ iridium oxides in which the energy scales of electron hopping, Coulomb interaction, and spin-orbit coupling are comparable. The members of the iridate Ruddlesden-Popper series $\text{Sr}_{n+1}\text{Ir}_n\text{O}_{3n+1}$ are of particular interest. In the $n = 1$ and $n = 2$ members of the series, the electronic correlations in concert with the strong spin-orbit coupling were found to lead to the formation of an effective total angular momentum $J_{\text{eff}} = 1/2$ Mott state²⁻⁷. Subsequent theoretical and experimental studies on charge carrier doped Sr_2IrO_4 revealed the signatures of the pseudogap and d -wave superconductivity⁸⁻¹⁵, which implies an importance of electronic correlations in Sr_2IrO_4 system.

In contrast, the role of electronic correlations in bilayered $\text{Sr}_3\text{Ir}_2\text{O}_7$ system is under intense debate. A neutron scattering experiments showed nearly identical ordered magnetic moments of $\text{Sr}_3\text{Ir}_2\text{O}_7$ and Sr_2IrO_4 , suggesting a similar strength of the electronic correlations in the two compounds^{16,17}. A scanning tunneling spectroscopy (STS) experiment of $\text{Sr}_3\text{Ir}_2\text{O}_7$ in combination with density-functional-theory (DFT) calculations suggested a critical role of electronic correlations in the formation of a substantial charge gap of about 130 meV¹⁸. The STS data further showed that the oxygen-vacancy-induced electronic structure changes were reminiscent of the filling-controlled Mott transitions in $3d/4d$ transition metal oxides. On the other hand, an angle-resolved photoemission spectroscopy (ARPES) experiment suggested a conventional Fermi-liquid state of $(\text{Sr}_{1-x}\text{La}_x)_3\text{Ir}_2\text{O}_7$ with a small mass renormalization of about 2¹⁹. Band structure calculations also suggested that $\text{Sr}_3\text{Ir}_2\text{O}_7$ might be almost a band insulator¹⁹⁻²². A tight-binding calculation predicted that a direct gap between the bands mainly composed of the $J_{\text{eff}} = 1/2$ states occurred at every momentum point and the Fermi level was found to barely touch the bottom of the occupied bands and the top of the unoccupied bands. Electronic correlations merely pushed the bands away from the Fermi level leading to the insulating state²².

Our paper provides experimental evidences of strong electronic correlations in $(\text{Sr}_{1-x}\text{La}_x)_3\text{Ir}_2\text{O}_7$. We investigated the electronic response of $(\text{Sr}_{1-x}\text{La}_x)_3\text{Ir}_2\text{O}_7$ by using infrared spectroscopy. We found that electron doping led to an insulator-metal transition that is reminiscent of the Mott transitions in strongly correlated $3d/4d$ transition metal oxides. We observed a spectral weight transfer from high energies to the ingap region to fill the charge gap of the parent compound. The intraband conductivity of the electron-doped compounds was found to be composed of a coherent and an incoherent responses. The sum rule and the extended Drude model analyses of our optical conductivity data revealed a substantial mass enhancement of the charge carriers in the metallic compound.

¹Department of Physics, Hanyang University, Seoul 04763, Korea. ²Department of Physics, Boston College, Chestnut Hill, Massachusetts 02467, USA. ³Department of Materials, University of California, Santa Barbara, California 93106, USA. Correspondence and requests for materials should be addressed to S.J.M. (email: soonjmoon@hanyang.ac.kr)

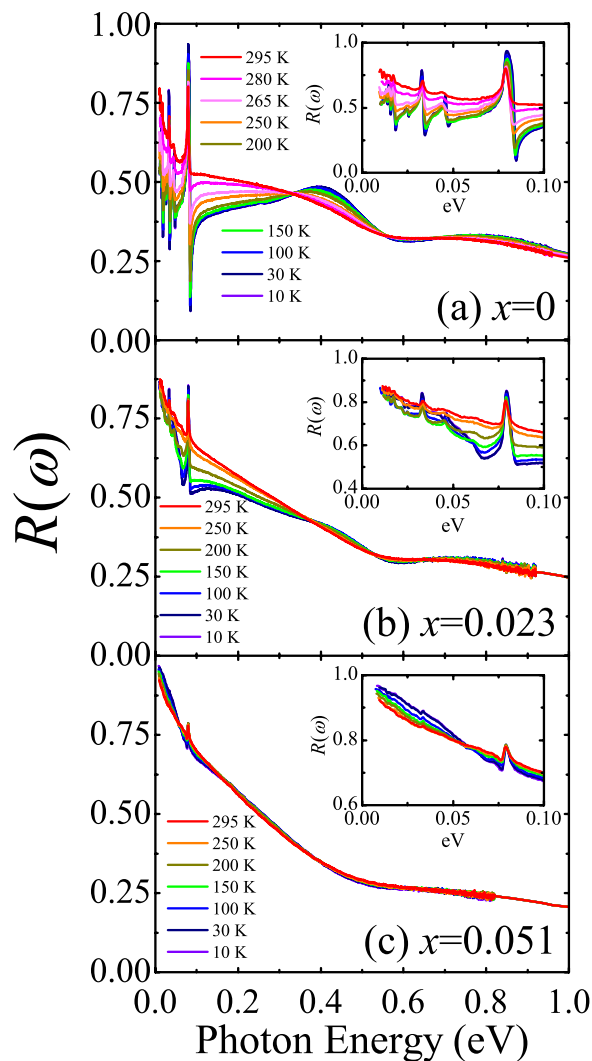


Figure 1. Temperature-dependent reflectivity spectra $R(\omega)$ of (a) $\text{Sr}_3\text{Ir}_2\text{O}_7$ ($x=0$), (b) $(\text{Sr}_{0.977}\text{La}_{0.023})_3\text{Ir}_2\text{O}_7$ ($x=0.023$), and (c) $(\text{Sr}_{0.949}\text{La}_{0.051})_3\text{Ir}_2\text{O}_7$ ($x=0.051$). Insets: $R(\omega)$ below 0.1 eV.

Results and Discussion

Figure 1 displays the reflectivity spectra $R(\omega)$ of $(\text{Sr}_{1-x}\text{La}_x)_3\text{Ir}_2\text{O}_7$. The reflectivity data show that the electron doping induces an insulator-metal transition. Insulating behavior is evident in $R(\omega)$ of $\text{Sr}_3\text{Ir}_2\text{O}_7$. At 10 K, the far-infrared reflectivity is dominated by sharp peaks which originate from infrared-active phonons as shown in Fig. 1(a). As temperature increases, $R(\omega)$ below 0.3 eV is enhanced accompanying a change in its slope; at higher temperatures $R(\omega)$ rises toward lower frequency implying the onset of an electronic contribution due to thermally-induced carriers²³. Two broad peaks at about 0.4 and 0.8 eV represent the optical excitations between the J_{eff} bands, which will be discussed in detail later. Upon electron doping, the absolute magnitude of $R(\omega)$ below 0.3 eV is enhanced and the peak structure at about 0.4 eV is suppressed [Fig. 1(b,c)]. The spectral shape of the low-temperature $R(\omega)$ also changes with doping; $R(\omega)$ below 0.3 eV of the La-doped compounds increases toward lower frequency, which is in sharp contrast to the spectral shape of $R(\omega)$ of the parent compound. These observations indicate the existence of itinerant carriers in the doped materials.

Insight into the evolution of the electronic response with electron doping can be gained from the analysis of optical conductivity data. Figure 2 shows the real part of the optical conductivity spectra $\sigma_1(\omega)$ of $(\text{Sr}_{1-x}\text{La}_x)_3\text{Ir}_2\text{O}_7$. The conductivity data of the parent compound $\text{Sr}_3\text{Ir}_2\text{O}_7$ can be interpreted in terms of the $J_{\text{eff}}=1/2$ Mott state⁴. The two peaks labeled as α and β in Fig. 2(a) correspond to the optical transitions to the $J_{\text{eff}}=1/2$ upper Hubbard band from the $J_{\text{eff}}=1/2$ lower Hubbard band and from the $J_{\text{eff}}=3/2$ band, respectively. The direct optical gap of $\text{Sr}_3\text{Ir}_2\text{O}_7$ at 10 K is estimated to be about 0.3 eV. The optical gap decreases progressively with increasing temperature accompanying the spectral weight transfer from the energy region above 0.3 eV to lower energies. This temperature dependence was attributed to the enhancement of the phonon-assisted optical excitations²³.

Electron doping prompts the collapse of the Mott gap. The optical transitions inherent to the $J_{\text{eff}}=1/2$ Mott state, i.e., the peaks α and β are depressed upon electron doping. The spectral weight removed from the high energies (>0.3 eV) is shifted to the energy region below the optical gap of the parent compound thus filling the

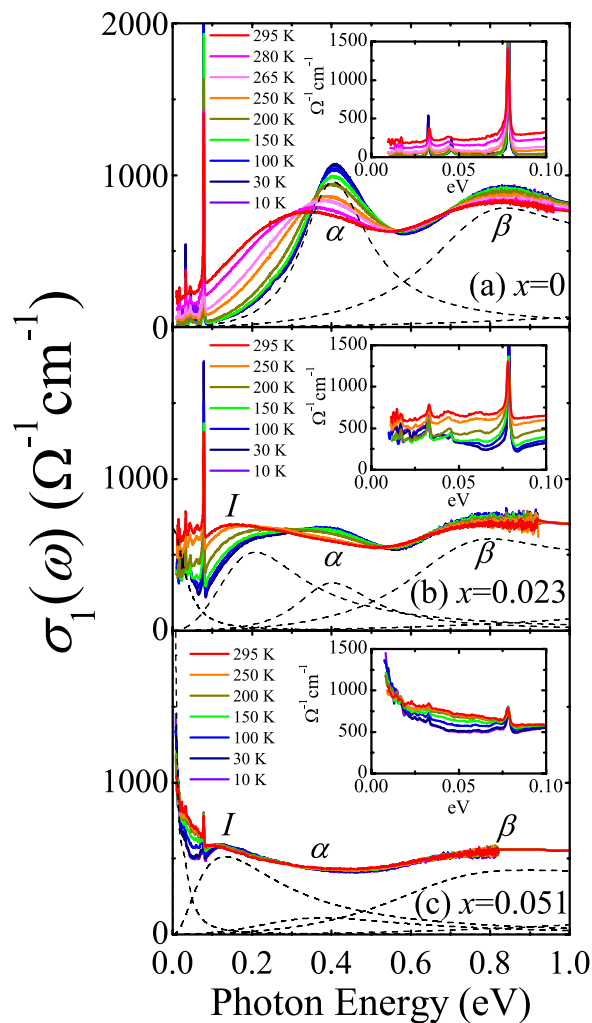


Figure 2. Real part of the optical conductivity spectra $\sigma_1(\omega)$ of (a) $\text{Sr}_3\text{Ir}_2\text{O}_7$ ($x=0$), (b) $(\text{Sr}_{0.977}\text{La}_{0.023})_3\text{Ir}_2\text{O}_7$ ($x=0.023$), and (c) $(\text{Sr}_{0.949}\text{La}_{0.051})_3\text{Ir}_2\text{O}_7$ ($x=0.051$). Dashed lines represent the oscillators used to fit $\sigma_1(\omega)$ at 10 K. We note that the oscillator labeled as β is composed of two Lorentzians. Insets: $\sigma_1(\omega)$ below 0.1 eV.

Mott gap. In $(\text{Sr}_{0.977}\text{La}_{0.023})_3\text{Ir}_2\text{O}_7$ the spectral weight forms a localized mode centered at about 0.18 eV along with a featureless conductivity below 0.1 eV, as shown in Fig. 2(b). This indicates an incoherent nature of the charge transport in $(\text{Sr}_{0.977}\text{La}_{0.023})_3\text{Ir}_2\text{O}_7$. The conductivity below about 0.05 eV increases slightly when the temperature is lowered across 150 K, which is consistent with the temperature dependence of the resistivity data¹⁷. We note that the temperature evolution of $\sigma_1(\omega)$ of $(\text{Sr}_{0.977}\text{La}_{0.023})_3\text{Ir}_2\text{O}_7$, i.e., the enhancement of the conductivity below 0.3 eV with the spectral weight transfer from high to low energies, is essentially the same as that of the parent compound.

Further electron doping leads to the development of a coherent electronic response at the expense of the peaks α and β . The conductivity data of $(\text{Sr}_{0.949}\text{La}_{0.051})_3\text{Ir}_2\text{O}_7$ shown in Fig. 2(c) clearly exhibit a Drude-like peak centered at $\omega=0$ eV. The Drude-like response becomes narrower with the lowering of temperature, resulting in the enhancement of the conductivity at the lowest energies continued to the DC value. This temperature dependence is qualitatively different from those of $\sigma_1(\omega)$ of $\text{Sr}_3\text{Ir}_2\text{O}_7$ and $(\text{Sr}_{0.977}\text{La}_{0.023})_3\text{Ir}_2\text{O}_7$. In the latter compounds, the conductivity at the lowest energies is suppressed with decreasing temperature. The spectral shape and the temperature dependence of $\sigma_1(\omega)$ thus clearly demonstrate a coherent metallic character of $(\text{Sr}_{0.949}\text{La}_{0.051})_3\text{Ir}_2\text{O}_7$.

In order to obtain detailed information on the changes in the energies and the spectral weights of the optical excitations with electron doping, we analyzed $\sigma_1(\omega)$ of $(\text{Sr}_{1-x}\text{La}_x)_3\text{Ir}_2\text{O}_7$ at 10 K by using the Drude-Lorentz oscillator model^{24,25}:

$$\sigma_1(\omega) = \frac{1}{4\pi} \frac{S_D \gamma_D}{\omega^2 + \gamma_D^2} + \frac{1}{4\pi} \sum_j \frac{S_j \gamma_j \omega^2}{(\omega_j^2 - \omega^2)^2 + \gamma_j^2 \omega^2}. \quad (1)$$

The first term represents the contribution from the Drude response. S_D and γ_D denote the strength and the scattering rate of the Drude peak. The second term corresponds to bound excitations. S_j , ω_j and γ_j are the strength, resonance frequency, and the width of the j th Lorentz oscillator, respectively. The coherent response of $(\text{Sr}_{1-x}\text{La}_x)_3\text{Ir}_2\text{O}_7$ cannot be explained in terms of a simple Drude oscillator, which is a typical characteristic

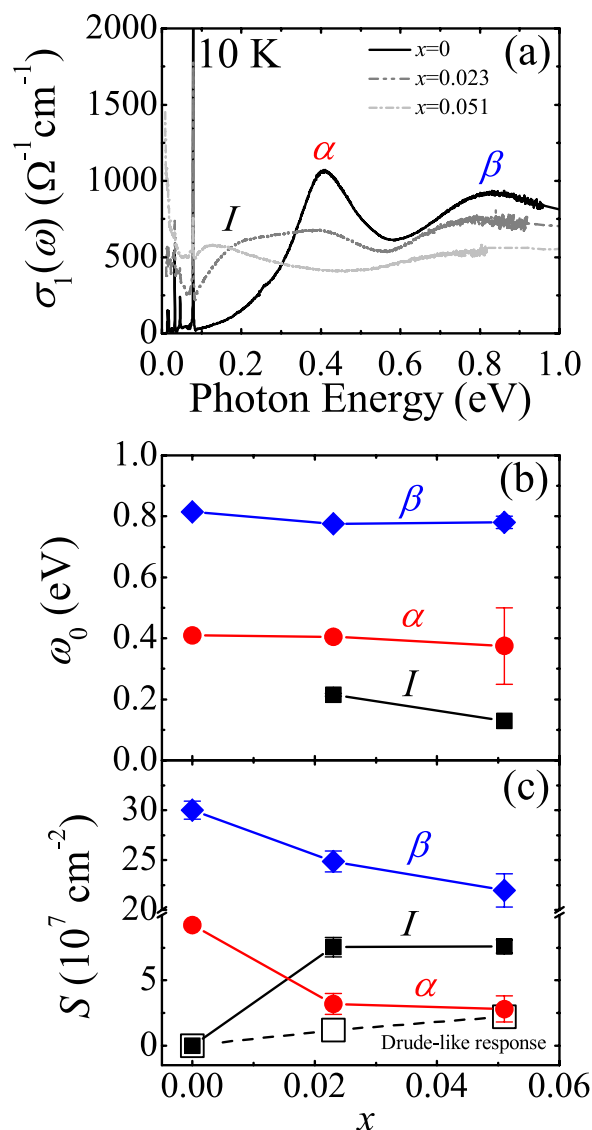


Figure 3. (a) $\sigma_1(\omega)$ of $(\text{Sr}_{1-x}\text{La}_x)_3\text{Ir}_2\text{O}_7$ at 10 K. (b) Resonant frequencies of the peaks I (solid squares), α (solid circles), and β (solid diamonds). (c) Strengths of the Drude-like response (open squares), the peaks I , α , and β .

of correlated electron materials. We used a combination of a Drude and a Lorentz oscillators to fit the coherent response located at $\omega < 0.05$ eV. We stress that the accurate information on the bare electronic structure can be gained from the analysis of $\sigma_1(\omega)$ at the lowest temperature 10 K. As shown in Fig. 2(a,b), the conductivity spectra at high temperatures are significantly different from the data at 10 K. The increase in temperature leads to the filling of the optical gap as well as the redshift of the peak α . This behavior was found not to be associated with the changes in the bare electronic structure but with the variation of the contribution from the thermal carriers²³.

Figure 3 summarizes the evolution of the electronic structure with electron doping. The comparison of $\sigma_1(\omega)$ at 10 K in Fig. 3(a) clearly illustrates the changes in the electronic structure; the suppression of the peaks α and β and the filling of the gap with ingap excitations (peak I) and a Drude-like response. In $(\text{Sr}_{0.977}\text{La}_{0.023})_3\text{Ir}_2\text{O}_7$, the incoherent response dominates the far-infrared conductivity. Conversely a coherent Drude-like response appears in the lowest energy region (< 0.05 eV) of $\sigma_1(\omega)$ of $(\text{Sr}_{0.949}\text{La}_{0.051})_3\text{Ir}_2\text{O}_7$. From the Drude-Lorentz model analysis, we find that the spectral weight transfer relevant to the insulator-metal transition occurs in the energy region where the optical transitions between the J_{eff} states are the main contributors to $\sigma_1(\omega)$. We also find that the energy values of the peaks α and β barely change with electron doping. This indicates that the Mott gap does not shift much in energy with doping. The peak I on the other hand exhibits sizeable redshift of about 0.08 eV and is likely to be merged into the coherent response at higher doping levels.

The evolution of $\sigma_1(\omega)$ of $(\text{Sr}_{1-x}\text{La}_x)_3\text{Ir}_2\text{O}_7$ bears significant similarities to the filling-controlled Mott transition in strongly correlated materials such as 3d and 4d transition metal oxides^{1,26}. The universal characteristics of the filling-controlled Mott metal-insulator transition in the context of infrared data include the following attributes: (i) The Mott gap excitation, i.e., the peak α , does not shift in energy appreciably but its intensity is suppressed^{26–28}. The energy region below the gap is filled up with states in the metallic side of the transition. (ii) The optical

conductivity contains a sizeable incoherent component before a fully coherent electronic response develops with the merger between the coherent and the incoherent contributions^{26,29–31}. The renormalization of the response from the itinerant carriers and the resulting development of an incoherent response is a fundamental behavior of the optical spectra of Mott transition systems. Our conductivity data shown in Figs 2 and 3 clearly display the features associated with the Mott transition and therefore suggest the crucial importance of electronic correlations in the $(\text{Sr}_{1-x}\text{La}_x)_3\text{Ir}_2\text{O}_7$ system.

A hallmark of strong electronic correlations is a substantial enhancement of the effective mass of the itinerant carriers of metallic compounds near the boundary of the metal-insulator transition^{1,26,32}. Having observed the spectroscopic signatures of the electronic correlations, we now estimate the mass enhancement to quantify the degree of the electronic correlations in $(\text{Sr}_{0.949}\text{La}_{0.051})_3\text{Ir}_2\text{O}_7$ by applying a sum rule to $\sigma_1(\omega)$. As a dimensionless measure of spectral weight, we calculate the effective electron number $N_{\text{eff}}(\omega)$ ²⁶ by using

$$N_{\text{eff}}(\omega) = \frac{2m_e V}{\pi e^2} \int_0^\omega \sigma_1(\omega') d\omega', \quad (2)$$

where m_e is the free electron mass and V is the volume containing one Ir^{4+} ion. If the high-frequency cutoff ω_c of the integral is chosen to include only the intraband contribution to $\sigma_1(\omega)$, then

$$N_{\text{eff,intra}}(\omega_c) = \frac{N}{(m_b/m_e)}, \quad (3)$$

where m_b is a band mass and N is the number of itinerant carriers or band filling^{26,33}. For correlated electron materials, the intraband response from the itinerant carriers is expected to separate into coherent and incoherent components due to many-body effects^{1,26}. The former corresponds to the Drude-like mode centered at $\omega = 0$ eV. If the high-frequency cutoff of the integral in equation (2) is chosen to contain the coherent component of the itinerant response, then

$$N_{\text{eff,coherent}}(\omega_c) = \frac{N}{(m^*/m_e)}, \quad (4)$$

where m^* is the effective mass^{26,33}.

In metallic $(\text{Sr}_{0.949}\text{La}_{0.051})_3\text{Ir}_2\text{O}_7$, the nominal number of itinerant electrons N should be $3x/2 = 0.0765$. The effective number of electrons responsible for the intraband conductivity $N_{\text{eff,intra}}$ can be estimated from equation (3) with $\omega_c = 0.37$ eV below which the Drude-like peak and ingap excitation are main contributors to the conductivity. The calculation gives $N_{\text{eff,intra}} \approx 0.057$, thus indicating $m_b \approx 1.3m_e$. The effective electron number associated with the coherent component can be calculated by choosing the high-frequency cutoff of equation (4) as 0.055 eV below which the Drude-like mode dominates the conductivity. The value of $N_{\text{eff,coherent}}$ is found to be about 0.014, yielding $m^* \approx 5.5m_e$. Our sum rule analysis therefore indicates a mass enhancement of $m^* \approx 4.2m_b$.

An alternative method of estimating the mass enhancement is the extended Drude model analysis. The extended Drude model where interacting systems are mapped into the free electron model with an effective mass introduces frequency-dependent mass enhancement^{26,34}

$$1 + \lambda(\omega) \equiv \frac{m^*(\omega)}{m_b} = \frac{\omega_p^2}{4\pi} \frac{\sigma_2(\omega)}{\omega[\sigma_1(\omega)^2] + [\sigma_2(\omega)^2]}, \quad (5)$$

where ω_p is the plasma frequency of the intraband response and $\sigma_2(\omega)$ ($\sigma_1(\omega)$) is an imaginary (real) part of the optical conductivity. The plasma frequency was calculated by using the relation $\omega_p^2 = 8 \int_0^{\omega_c} \sigma_1(\omega) d\omega$ with the high-frequency cutoff of $\omega_c = 0.37$ eV. As displayed in Fig. 4, the mass enhancement estimated from the extended Drude model analysis reaches about 6 at the lowest energy, which is close to the value from our sum rule analysis.

The mass enhancement of $(\text{Sr}_{1-x}\text{La}_x)_3\text{Ir}_2\text{O}_7$ from our analyses is comparable to those of strongly correlated $3d/4d$ transition metal oxides. For the cuprates, the mass enhancement ranges from 2 to $10^{30,35,36}$. The mass enhancement of VO_2 which is one of the representative examples of Mott system was about 5 near the metal-insulator transition³⁷. The perovskite titanates and vanadates were found to have the mass enhancement of about 4–12^{38–41}. A $4d$ itinerant ferromagnet SrRuO_3 had the mass enhancement of about 6⁴². Large mass enhancement of $(\text{Sr}_{0.949}\text{La}_{0.051})_3\text{Ir}_2\text{O}_7$ can be due to the formation of the very narrow $J_{\text{eff}} = 1/2$ bands near the Fermi level^{2,4}. Polaronic or excitonic effects could also contribute the mass enhancement^{26,43–47}. Previous spectroscopic experiments on Sr_2IrO_4 and $\text{Sr}_3\text{Ir}_2\text{O}_7$ suggested an importance of electron-phonon coupling. The electron-phonon coupling can induce a renormalization of intraband response and lead to the formation of an incoherent side band in the optical conductivity. The polaronic side band should show strong temperature evolutions^{26,43}. We note that the ingap excitation in $\sigma_1(\omega)$ of $(\text{Sr}_{0.949}\text{La}_{0.051})_3\text{Ir}_2\text{O}_7$ displays negligible temperature dependence, indicating a minimal role of the electron-phonon coupling. Therefore our result indicates that the electronic correlations in $(\text{Sr}_{1-x}\text{La}_x)_3\text{Ir}_2\text{O}_7$ are as strong as those in $3d/4d$ transition metal oxides and play a critical role in the charge dynamics of $(\text{Sr}_{1-x}\text{La}_x)_3\text{Ir}_2\text{O}_7$.

Conclusion

We investigated the electronic response of the $(\text{Sr}_{1-x}\text{La}_x)_3\text{Ir}_2\text{O}_7$ system by using infrared spectroscopy. A filling-controlled insulator-metal transition revealed in our optical conductivity data bore striking similarities with those of strongly correlated electron matters such as $3d/4d$ transition metal oxides. The sum rule and the extended Drude model analyses further revealed a substantial mass enhancement of the itinerant carriers of the

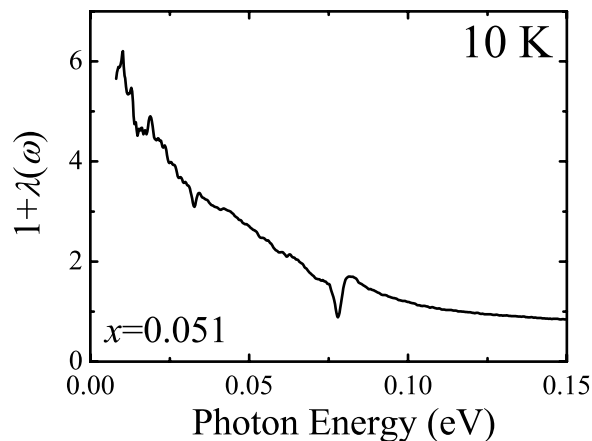


Figure 4. Mass enhancement of $(\text{Sr}_{0.949}\text{La}_{0.051})_3\text{Ir}_2\text{O}_7$ at 10 K calculated from the extended Drude model analysis.

metallic compound near the metal-insulator transition boundary. Our experimental data obtained by using a bulk-sensitive probe and the model-independent analyses demonstrate a critical role of the electronic correlations in the $(\text{Sr}_{1-x}\text{La}_x)_3\text{Ir}_2\text{O}_7$ system.

Methods

Single-crystals of $(\text{Sr}_{1-x}\text{La}_x)_3\text{Ir}_2\text{O}_7$ ($x = 0, 0.023$ and 0.051) were grown via flux techniques. Dopant content was determined by energy-dispersive x-ray spectroscopy measurements. Details of the growth procedure were described elsewhere¹⁷.

We measured the *ab*-plane reflectivity spectra $R(\omega)$ in the photon energy region between 5 meV and 1 eV using a Fourier transform infrared spectrometer (Bruker VERTEX 70v). An *in-situ* gold overcoating technique⁴⁸ was used to compensate the effect of rough sample surfaces. The dielectric constants, $\varepsilon = \varepsilon_1 + i\varepsilon_2$, in the energy range from 0.74 to 5 eV were obtained by using spectroscopic ellipsometer (V-VASE, J. A. Woollam Co.). For the low-energy spectra below 5 meV, $R(\omega)$ was extrapolated by using the Hagen-Rubens relation²⁴. We transformed $R(\omega)$ to obtain the complex conductivity $\sigma(\omega) = \sigma_1(\omega) + i\sigma_2(\omega)$ through the Kramers-Kronig analysis.

References

- Imada, M., Fujimori, A. & Tokura, Y. Metal-insulator transitions. *Rev. Mod. Phys.* **70**, 1039–1263 (1998).
- Kim, B. J. *et al.* Novel $J_{\text{eff}} = 1/2$ Mott State Induced by Relativistic Spin-Orbit Coupling in Sr_2IrO_4 . *Phys. Rev. Lett.* **101**, 076402 (2008).
- Kim, B. J. *et al.* Phase-Sensitive Observation of a Spin-Orbital Mott State in Sr_2IrO_4 . *Science* **323**, 1329–1332 (2009).
- Moon, S. J. *et al.* Dimensionality-Controlled Insulator-Metal Transition and Correlated Metallic State in 5d Transition Metal Oxides $\text{Sr}_{n+1}\text{Ir}_n\text{O}_{3n+1}$ ($n = 1, 2, \infty$). *Phys. Rev. Lett.* **101**, 226402 (2008).
- Kim, J. *et al.* Magnetic Excitation Spectra of Sr_2IrO_4 Probed by Resonant Inelastic X-Ray Scattering: Establishing Links to Cuprate Superconductors. *Phys. Rev. Lett.* **108**, 177003 (2012).
- Fujiyama, S. *et al.* Two-Dimensional Heisenberg Behavior of $J_{\text{eff}} = 1/2$ Isospins in the Paramagnetic State of the Spin-Orbital Mott Insulator Sr_2IrO_4 . *Phys. Rev. Lett.* **108**, 247212 (2012).
- Hsieh, D., Mahmood, F., Torchinsky, D. H., Cao, G. & Gedik, N. Observation of a metal-to-insulator transition with both Mott-Hubbard and Slater characteristics in Sr_2IrO_4 from time-resolved photocarrier dynamics. *Phys. Rev. B* **86**, 035128 (2012).
- Wang, F. & Senthil, T. Twisted Hubbard Model for Sr_2IrO_4 : Magnetism and Possible High Temperature Superconductivity. *Phys. Rev. Lett.* **106**, 136402 (2011).
- Watanabe, H., Shirakawa, T. & Yunoki, S. Monte Carlo Study of an Unconventional Superconducting Phase in Iridium Oxide $J_{\text{eff}} = 1/2$ Mott Insulators Induced by Carrier Doping. *Phys. Rev. Lett.* **110**, 027002 (2013).
- Meng, Z. Y., Kim, Y. B. & Kee, H.-Y. Odd-Parity Triplet Superconducting Phase in Multiorbital Materials with a Strong Spin-Orbit Coupling: Application to Doped Sr_2IrO_4 . *Phys. Rev. Lett.* **113**, 177003 (2014).
- Kim, Y. K. *et al.* Fermi arcs in a doped pseudospin-1/2 Heisenberg antiferromagnet. *Science* **345**, 187–190 (2014).
- Kim, Y. K., Sung, N. H., Denlinger, J. D. & Kim, B. J. Observation of a *d*-wave gap in electron-doped Sr_2IrO_4 . *Nat. Phys.* **12**, 37–41 (2016).
- Yan, Y. J. *et al.* Electron-Doped Sr_2IrO_4 : An Analogue of Hole-Doped Cuprate Superconductors Demonstrated by Scanning Tunneling Microscopy. *Phys. Rev. X* **5**, 041018 (2015).
- de la Torre, A. *et al.* Collapse of the Mott Gap and Emergence of a Nodal Liquid in Lightly Doped Sr_2IrO_4 . *Phys. Rev. Lett.* **115**, 176402 (2015).
- Cao, Y. *et al.* Hallmarks of the Mott-Metal Crossover in the Hole Doped $J = 1/2$ Mott insulator Sr_2IrO_4 . *arXiv:1406.4978* (2014).
- Dhital, C. *et al.* Neutron scattering study of correlated phase behavior in Sr_2IrO_4 . *Phys. Rev. B* **87**, 144405 (2013).
- Hogan, T. *et al.* First-Order Melting of a Weak Spin-Orbit Mott Insulator into a Correlated Metal. *Phys. Rev. Lett.* **114**, 257203 (2015).
- Okada, Y. *et al.* Imaging the evolution of metallic states in a correlated iridate. *Nat. Mater.* **12**, 707–713 (2013).
- De la Torre, A. *et al.* Coherent Quasiparticles with a Small Fermi Surface in Lightly Doped $\text{Sr}_3\text{Ir}_2\text{O}_7$. *Phys. Rev. Lett.* **113**, 256402 (2014).
- He, J. *et al.* Fermi Arcs vs. Fermi Pockets in Electron-doped Perovskite Iridates. *Sci. Rep.* **5**, 8533 (2015).
- He, J. *et al.* Spectroscopic evidence for negative electronic compressibility in a quasi-three-dimensional spin-orbit correlated metal. *Nat. Mater.* **14**, 577–582 (2015).
- Carter, J.-M. & Kee, H.-Y. Microscopic theory of magnetism in $\text{Sr}_3\text{Ir}_2\text{O}_7$. *Phys. Rev. B* **87**, 014433 (2013).
- Park, H. J. *et al.* Phonon-assisted optical excitation in the narrow bandgap Mott insulator $\text{Sr}_3\text{Ir}_2\text{O}_7$. *Phys. Rev. B* **89**, 155115 (2014).

24. Wooten, F. *Optical Properties of Solids* (Academic Press, New York, 1972).
25. Dressel, M. & Grüner, G. *Electrodynamics of Solids* (Cambridge University Press, Cambridge, England, 2002).
26. Basov, D. N., Averitt, R. D., van der Marel, D., Dressel, M. & Haule, K. Electrodynamic of correlated electron materials. *Rev. Mod. Phys.* **83**, 471–541 (2011).
27. Dagotto, E., Moreo, A., Ortolani, F., Poilblanc, D. & Riera, J. Static and dynamical properties of doped Hubbard clusters. *Phys. Rev. B* **45**, 10741–10760 (1992).
28. Pruschke, T., Cox, D. L. & Jarrell, M. Hubbard model at infinite dimensions: Thermodynamic and transport properties. *Phys. Rev. B* **47**, 3553–3565 (1993).
29. Katsufuji, T., Okimoto, Y. & Tokura, Y. Spectral Weight Transfer of the Optical Conductivity in Doped Mott Insulators. *Phys. Rev. Lett.* **75**, 3497–3500 (1995).
30. Uchida, S. *et al.* Optical spectra of $\text{La}_{2-x}\text{Sr}_x\text{CuO}_4$: Effect of carrier doping on the electronic structure of the CuO_2 plane. *Phys. Rev. B* **43**, 7942–7954 (1991).
31. Lee, J. S., Krockenberger, Y., Takahashi, K. S., Kawasaki, M. & Tokura, Y. Insulator-metal transition driven by change of doping and spin-orbit interaction in Sr_2IrO_4 . *Phys. Rev. B* **85**, 035101 (2012).
32. Brinkman, W. F. & Rice, T. M. Application of Gutzwiller's Variational Method to the Metal-Insulator Transition. *Phys. Rev. B* **2**, 4302–4304 (1970).
33. Orenstein, J. *et al.* Frequency- and temperature-dependent conductivity in $\text{YBa}_2\text{Cu}_3\text{O}_{6+x}$ crystals. *Phys. Rev. B* **42**, 6342–6362 (1990).
34. Puchkov, A. V., Basov, D. N. & Timusk, T. The pseudogap state in high- T_c superconductors: an infrared study. *J. Phys. Condens. Matter* **8**, 10049 (1996).
35. Onose, Y., Taguchi, Y., Ishizaka, K. & Tokura, Y. Charge dynamics in underdoped $\text{Nd}_{2-x}\text{Ce}_x\text{CuO}_4$: Pseudogap and related phenomena. *Phys. Rev. B* **69**, 024504 (2004).
36. Basov, D. N. *et al.* Unconventional energetics of the pseudogap state and superconducting state in high- T_c cuprates. *Phys. Rev. B* **63**, 134514 (2001).
37. Qazilbash, M. M. *et al.* Mott Transition in VO_2 Revealed by Infrared Spectroscopy and Nano-Imaging. *Science* **318**, 1750–1753 (2007).
38. Yoshida, T. *et al.* Photoemission spectral weight transfer and mass renormalization in the Fermi-liquid system $\text{La}_{1-x}\text{Sr}_x\text{TiO}_{3+y/2}$. *Europhys. Lett.* **59**, 258–264 (2002).
39. Taguchi, Y., Tokura, Y., Arima, T. & Inaba, F. Change of electronic structures with carrier doping in the highly correlated electron system $\text{Y}_{1-x}\text{Ca}_x\text{TiO}_3$. *Phys. Rev. B* **48**, 511–518 (1993).
40. Kasuya, M., Tokura, Y., Arima, T., Eisaki, H. & Uchida, S. Optical spectra of $\text{Y}_{1-x}\text{Ca}_x\text{VO}_3$: Change of electronic structures with hole doping in Mott-Hubbard insulators. *Phys. Rev. B* **47**, 6197–6202 (1993).
41. Fujishima, Y., Tokura, Y., Arima, T. & Uchida, S. Optical-conductivity spectra of $\text{Sr}_{1-x}\text{La}_x\text{TiO}_3$: Filling-dependent effect of the electron correlation. *Phys. Rev. B* **46**, 11167–11170 (1992).
42. Kostic, P. *et al.* Non-Fermi-Liquid Behavior of SrRuO_3 : Evidence from Infrared Conductivity. *Phys. Rev. Lett.* **81**, 2498–2501 (1998).
43. van Mechelen, J. L. M. *et al.* Electron-Phonon Interaction and Charge Carrier Mass Enhancement in SrTiO_3 . *Phys. Rev. Lett.* **100**, 226403 (2008).
44. Sohn, C. H. *et al.* Orbital-dependent polaron formation in the relativistic Mott insulator Sr_2IrO_4 . *Phys. Rev. B* **90**, 041105 (2014).
45. King, P. D. C. *et al.* Spectroscopic indications of polaronic behavior of the strong spin-orbit insulator $\text{Sr}_3\text{Ir}_2\text{O}_7$. *Phys. Rev. B* **87**, 241106 (2013).
46. Li, Y. *et al.* Giant optical enhancement of strain gradient in ferroelectric BiFeO_3 thin films and its physical origin. *Sci. Rep.* **5**, 16650 (2015).
47. Li, Y. *et al.* Strong lattice correlation of non-equilibrium quasiparticles in a pseudospin-1/2 Mott insulator Sr_2IrO_4 . *Sci. Rep.* **6**, 19302 (2016).
48. Homes, C. C., Reedyk, M., Cradles, D. A. & Timusk, T. Technique for measuring the reflectance of irregular, submillimeter-sized samples. *Appl. Opt.* **32**, 2976–2983 (1993).

Acknowledgements

This research was supported by Basic Science Research Program through the National Research Foundation of Korea (NRF) Funded by the Ministry of Science, ICT and Future Planning (2014R1A2A1A11054351). This work was supported in part by NSF Award No. DMR-1505549 (S.D.W.), as well as by the MRSEC Program of the National Science Foundation under Award No. DMR 1121053 (T.H.). Part of this study has been performed using facilities at IBS Center for Correlated Electron Systems, Seoul National University.

Author Contributions

G.H.A. and S.J.S. performed the experiments. Data analysis was carried out by G.H.A., S.J.M., T.H. and S.D.W. grew and characterized the single crystals. G.H.A. and S.J.M. wrote the manuscript and all the authors reviewed the manuscript. S.J.M. supervised the project.

Additional Information

Competing financial interests: The authors declare no competing financial interests.

How to cite this article: Ahn, G. *et al.* Infrared Spectroscopic Evidences of Strong Electronic Correlations in $(\text{Sr}_{1-x}\text{La}_x)_3\text{Ir}_2\text{O}_7$. *Sci. Rep.* **6**, 32632; doi: 10.1038/srep32632 (2016).



This work is licensed under a Creative Commons Attribution 4.0 International License. The images or other third party material in this article are included in the article's Creative Commons license, unless indicated otherwise in the credit line; if the material is not included under the Creative Commons license, users will need to obtain permission from the license holder to reproduce the material. To view a copy of this license, visit <http://creativecommons.org/licenses/by/4.0/>

© The Author(s) 2016